GRB jets

Miguel A. Aloy

ERC Fellow
Departamento de Astronomía y Astrofísica

VNIVERSITAT DE VALÈNCIA

collaborators
Carlos Cuesta-Martínez, M. Obergaulinger, P. Mimica,
T. Rembiasz, P. Cerdá-Durán, E. Müller

RIKEN GRB Workshop 2015

Tokyo, 1 – 09 - 2015

LGRB Progenitors: Collapsars

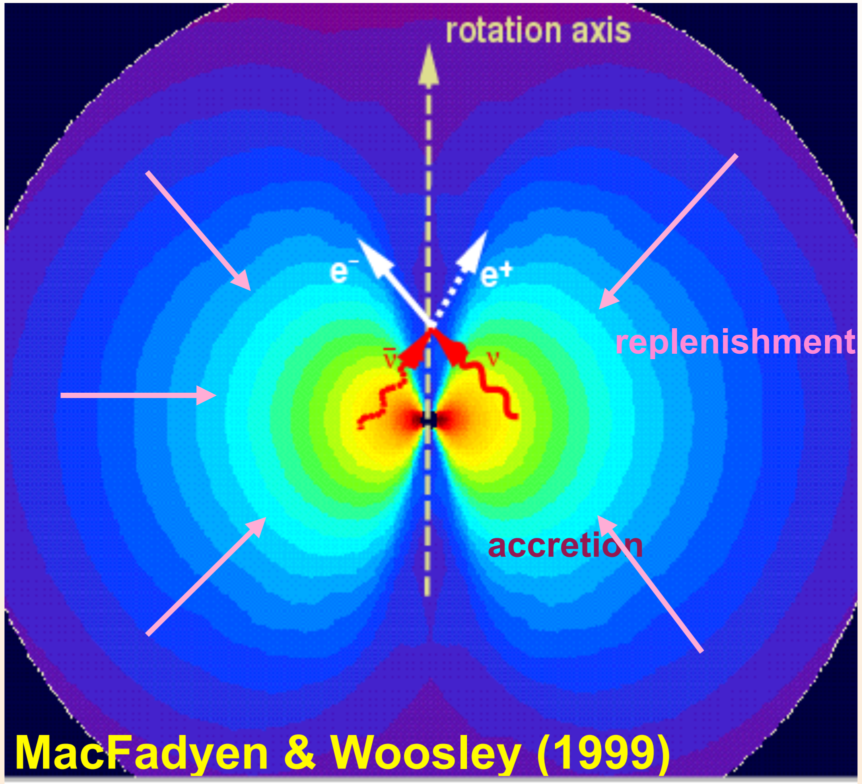

Woosley (1993):

– Collapse of a massive ($M_* \sim 30M_\odot$, WR) rotating star that does not form a successful SN but collapses to a BH ($M_{BH} \sim 3M_\odot$) surrounded by a thick accretion disk. The hydrogen envelope is lost by stellar winds, interaction with a companion, etc.

– The viscous accretion onto the BH ⇒ strong heating ⇒ thermal νν-annihilating preferentially around the axis ⇒ formation of a relativistic jet ($\Gamma=[1-(v/c)^2]^{-1/2}$).

– However, **the ability of producing thermally driven outflows with Γ≳100 is limited**

– Alternative generation: ***hydromagnetic*** (Blandford-Payne mechanism) or ***electromagnetic*** (Blandford-Znajek mechanism).

⇒ **the resulting outflow will be magnetized.**

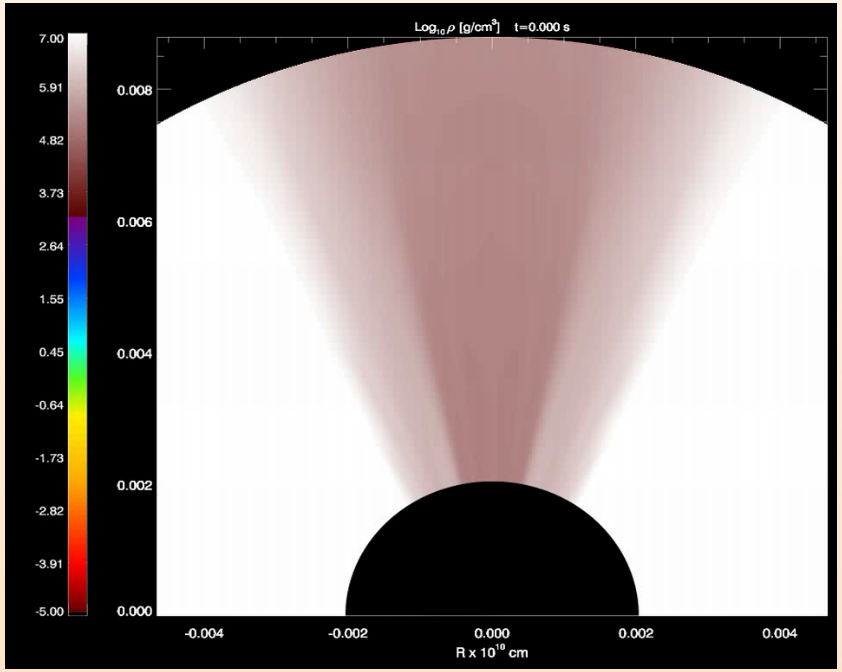

Aloy et al. (2000)

Why do we need B-fields to grow?

Blandford-Payne or Blandford Znajek mechanisms may account for the observed energetics ***IF HUGE B-fields develop in the stellar core***:

$$L_{BZ} = 1.7 \times 10^{51} a^2 \left(\frac{M_{BH}}{M_\odot}\right)^2 \left(\frac{B}{10^{15}\,G}\right)^2 \mathrm{erg\,s^{-1}}$$

Since we begin from massive stars with cores having WD-like configurations (B_0 ~10^8 - 10^9 G) ***we must amplify the initial (seed) B-field.***

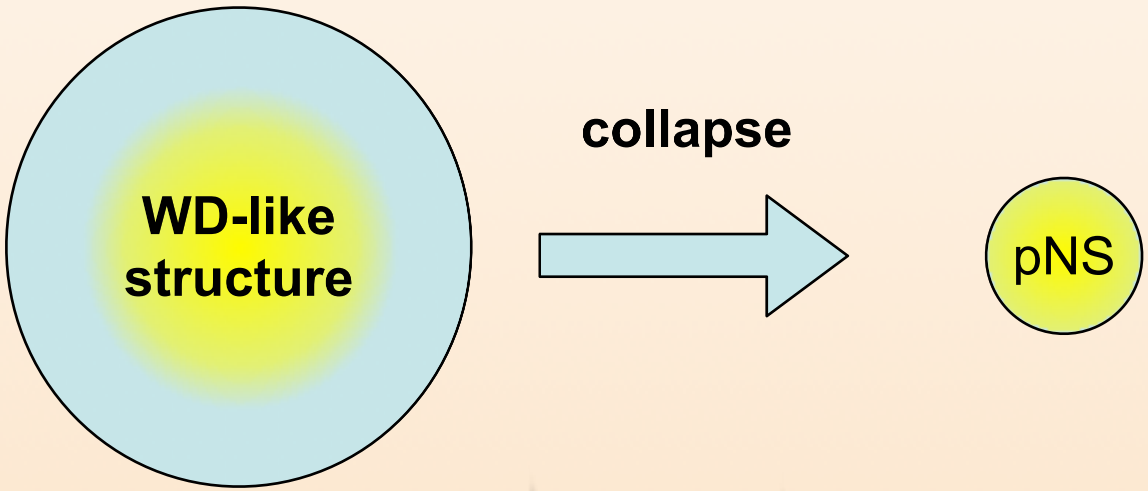

R~1000 km
B_0 ~ 10^9 G

B-flux conservation

R~10 km
B_c ~ 10^{13} G

but B_c << 10^{15} G ⇒ collapse insufficient

Why do we need B-fields to grow?

Blandford-Payne or Blandford Znajek mechanisms may account for the observed energetics ***<u>IF HUGE B-fields develop in the stellar core</u>***:

$$L_{BZ} = 1.7 \times 10^{51} a^2 \left(\frac{M_{BH}}{M_\odot}\right)^2 \left(\frac{B}{10^{15}\,G}\right)^2 \mathrm{erg\,s^{-1}}$$

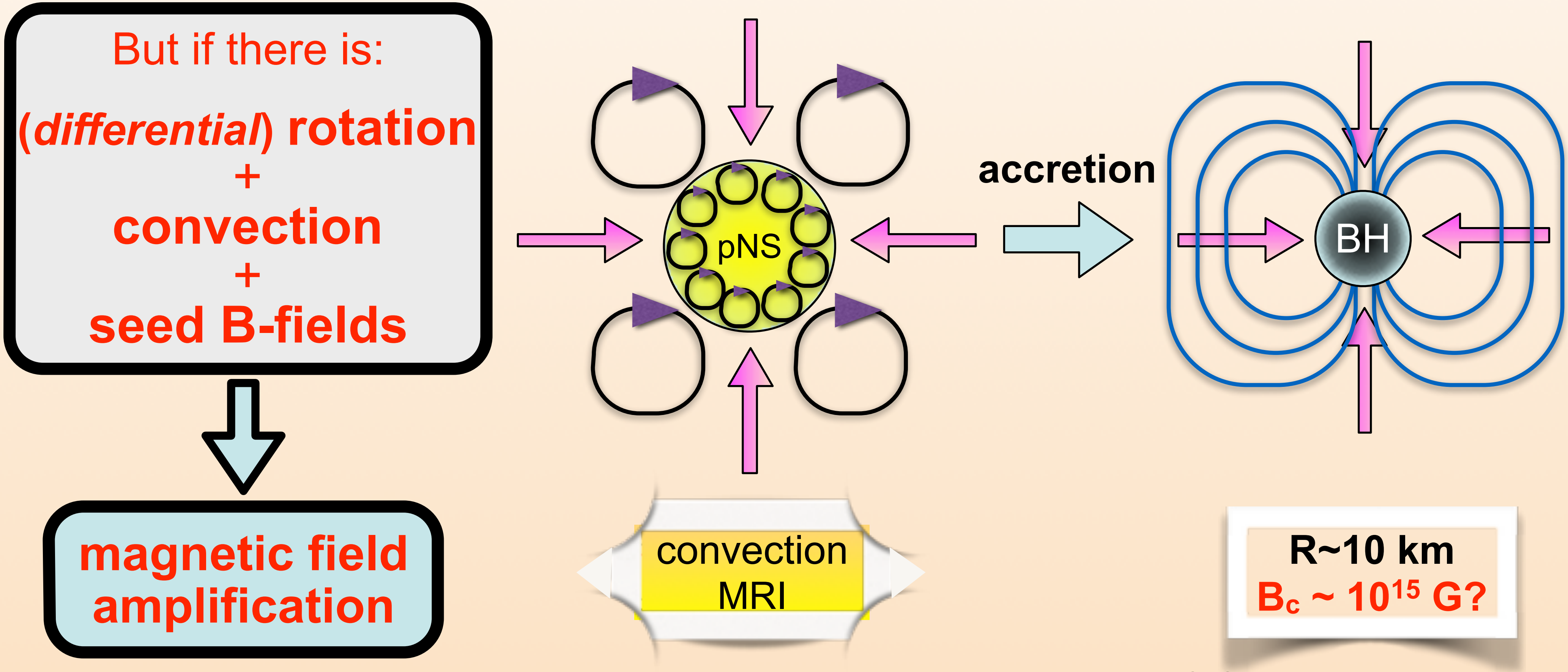

B-field growth in PNS and CC-SNe

- Field amplification by
  - Convection (unstable thermal stratification)
  - Magneto-rotational instability

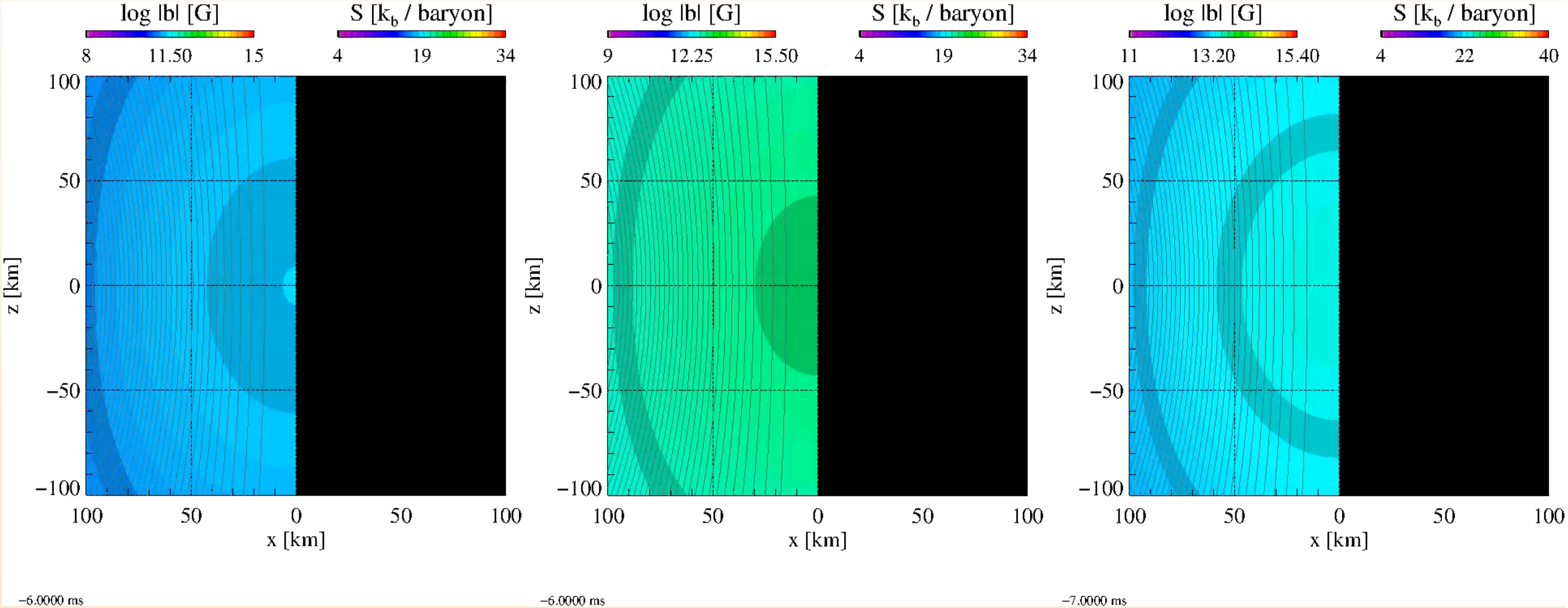

B10: The B-field does not change the dynamics of the core.

Obergaulinger, Janka & Aloy (2014)

B11.5: The B-field is strong enough to modify the post-shock flows. It suppresses the dissipation of bubbles, leading to an earlier predominance of large-scale bubbles and, consequently, an earlier onset of explosion.

B12: The post-shock region is always dominated by few very persistent large-scale bubbles, and the shock exhibits very regular, slow oscillations, which after only ~400 ms turn into a rapid shock expansion.

B-field growth in PNS and CC-SNe

- Field amplification by
  - Convection
  - Magneto-rotational instability

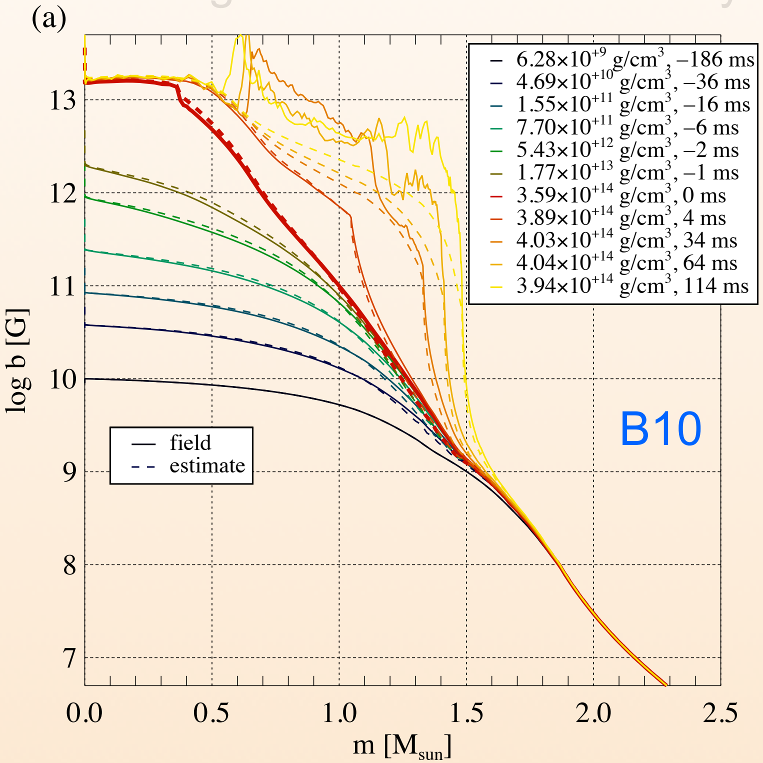

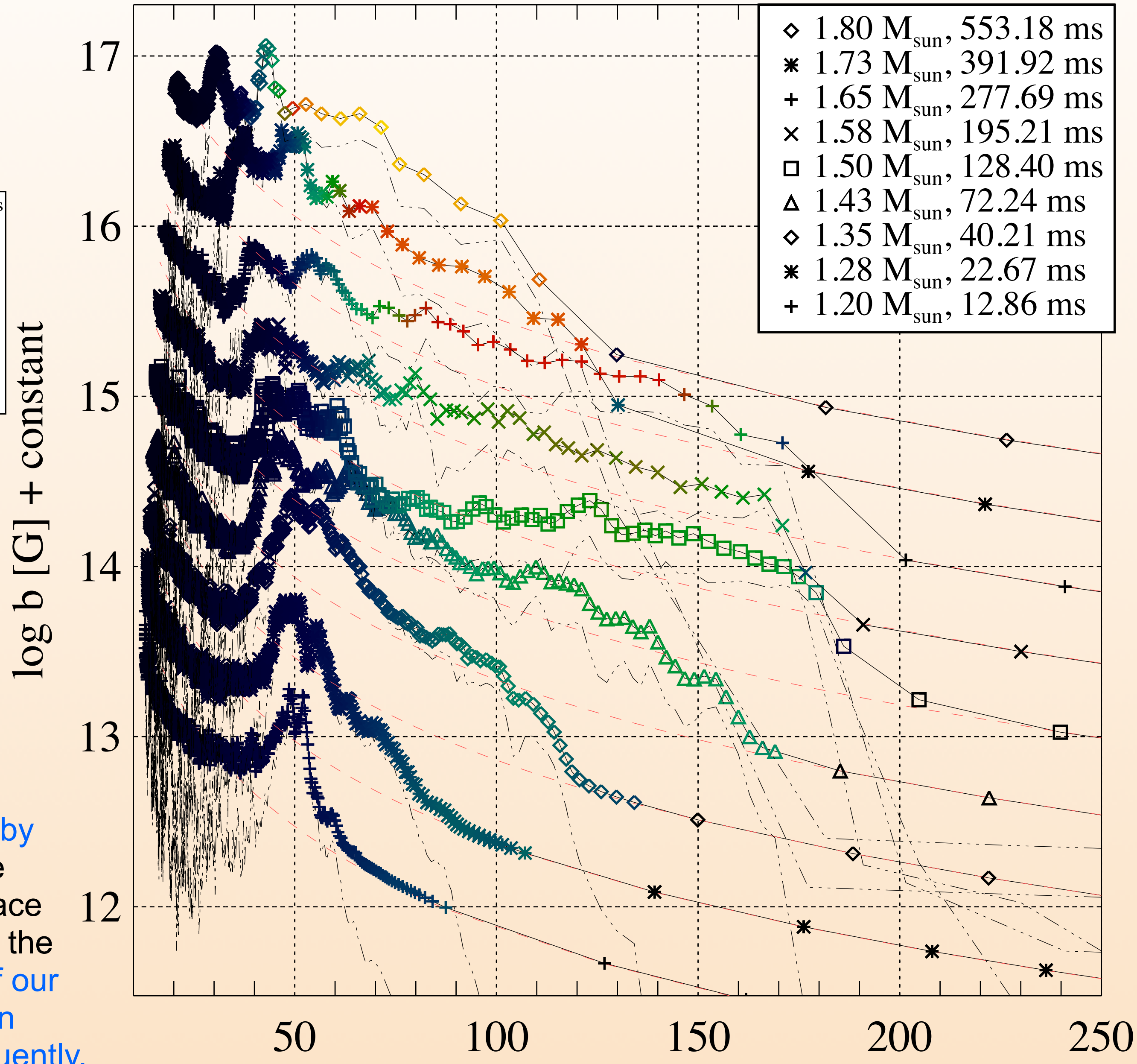

After bounce: Convection + SASI amplify by factors ~5 the B-field as a the result of the number of small-eddy turnovers taking place within the time scale of advection through the post-shock layer. Due to this limit, most of our models do not reach equipartition between kinetic and magnetic energy and, consequently, evolve similarly to the non-magnetic case.

Obergaulinger, a & Aloy (2014)

B-field saturation in PNS

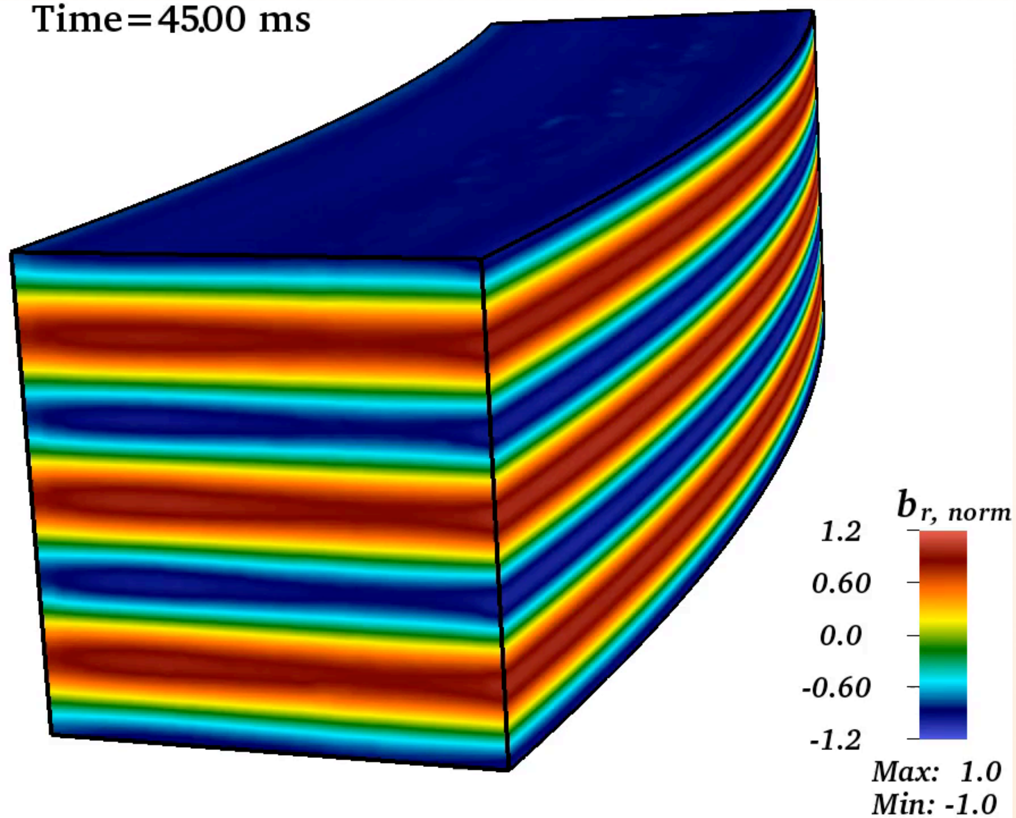

Rembiasz et al. (2015; arXiv:1508.04799):

(r,z,φ) = (100, 400, 100) or (200, 800, 200)

r x z x φ = 1 km x 4 km x 1 km

r_0 = 15.5 km

B_{z0} = 4.6 x 10^{13} G

λ_{MRI} = 0.33 km

$\nu = \eta$ = 4.45 x 10^8 cm^2/s

$\Omega = \Omega_0 \left(\frac{r_0}{r}\right)^q$

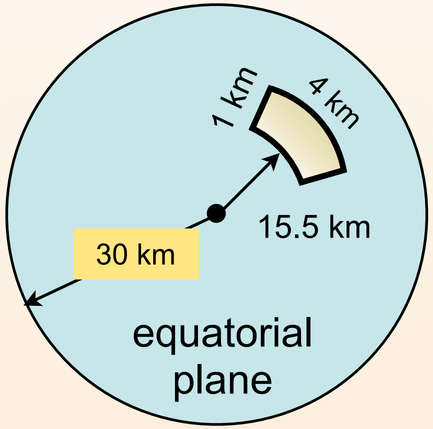

MRI exponential growth

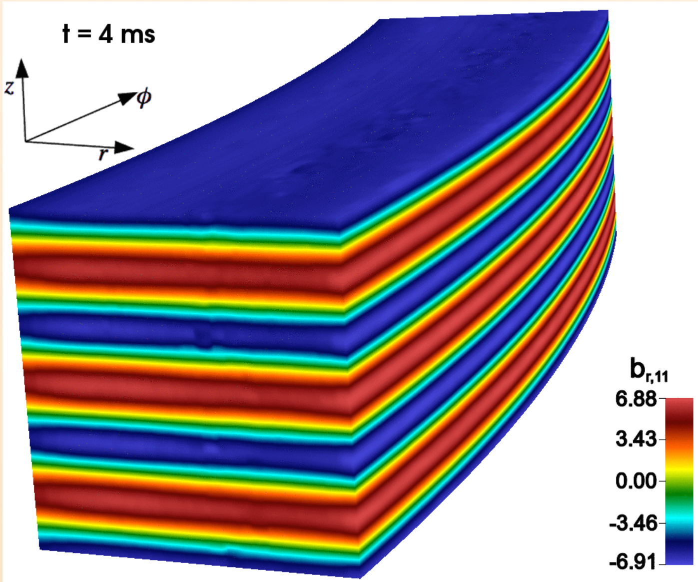

Parasites saturate the growth

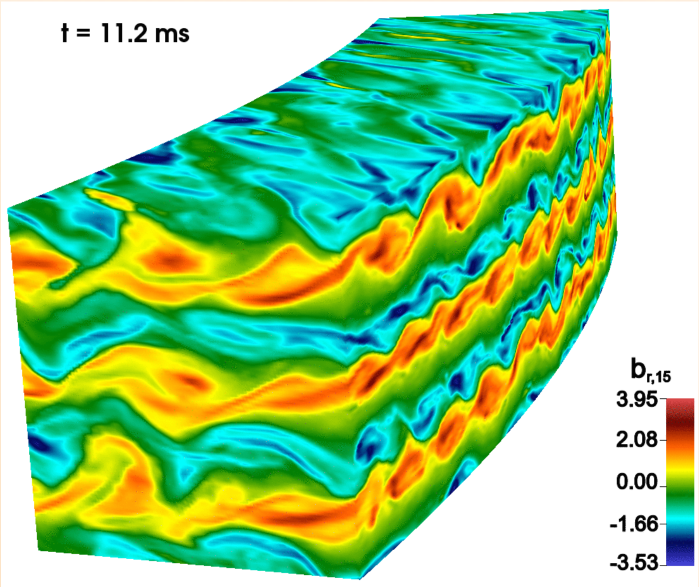

Final turbulent stage

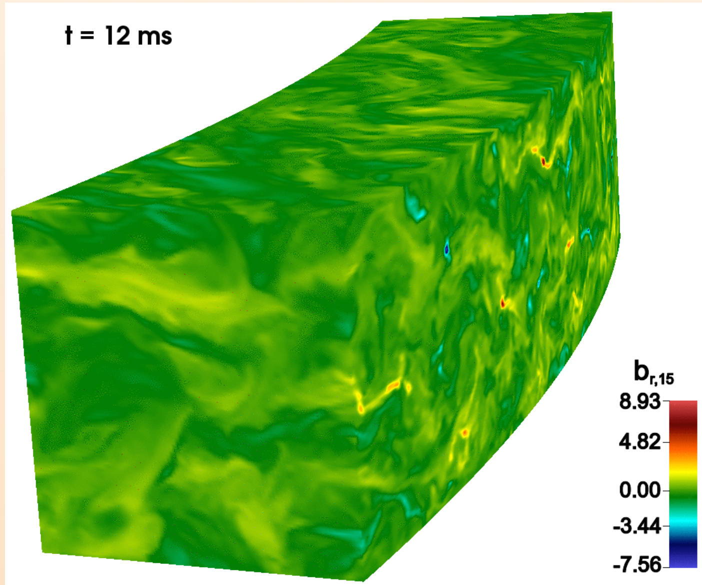

B-field saturation in PNS

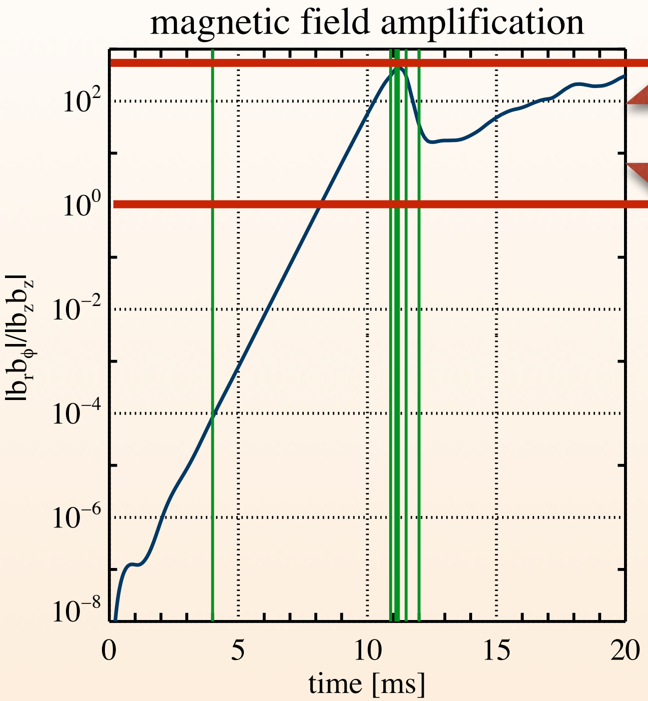

$B_{p,max}$ ~ 10^{15} G

AMPLIFICATION FACTOR ~ 20

B_{z0} = 4.6 x 10^{13} G

Rembiasz et al. (2015; arXiv:1508.04799)

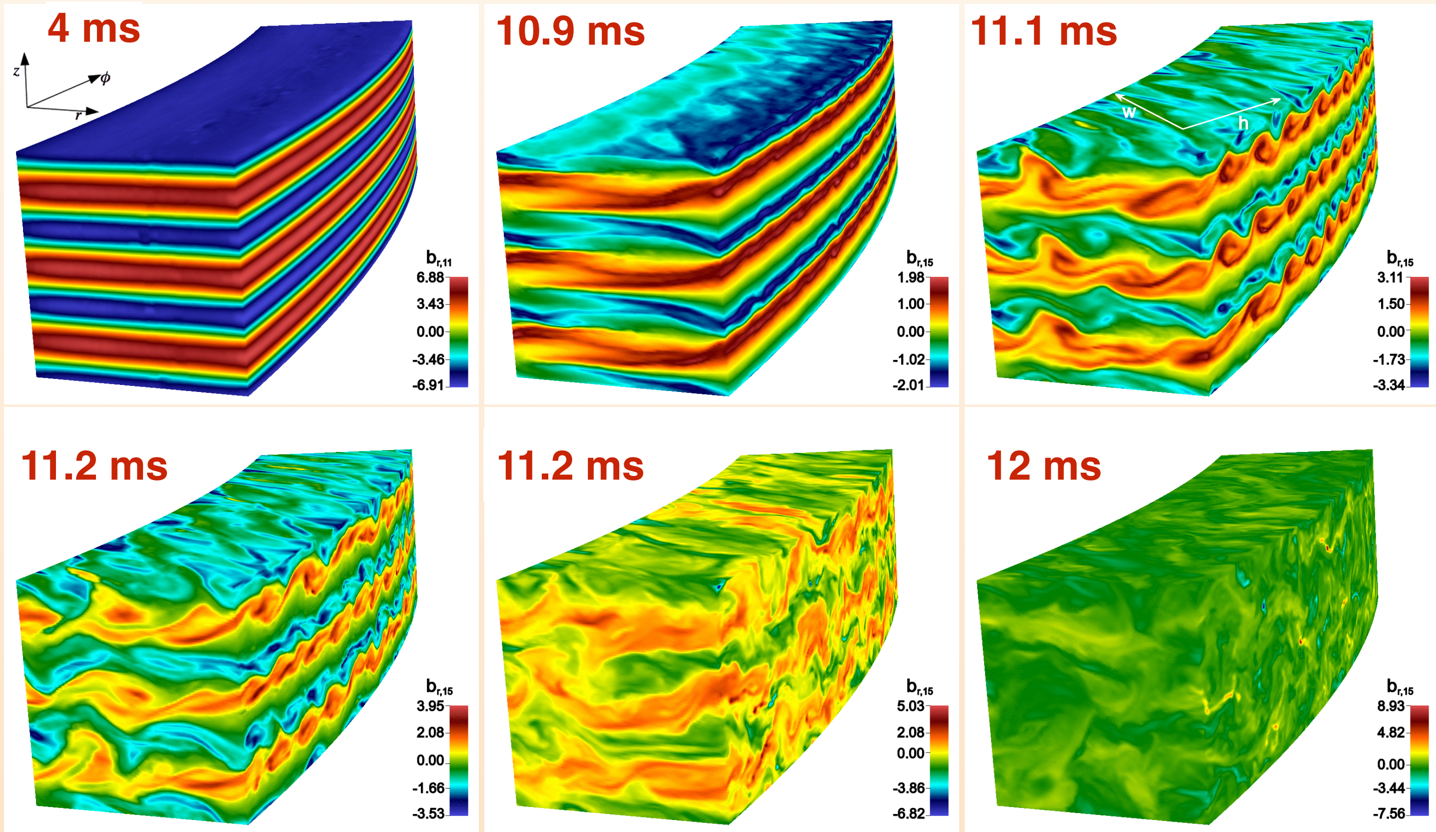

Figure 6. Radial component of the magnetic field of the three-dimensional MRI model 7 at six different times, which in Fig. 5 are marked by vertical lines.

For CCSNe, the parasitic instabilities are KH modes feeding off MRI channels, rather than tearing (resistive) modes.

Numerical set up

- Goal: **Compute the radiative signature of collapsar jets.**
- Two steps:
  1. ***RMHD models*** (this talk).
  2. Postprocessing and obtaining radiative signature (SPEV code; Mimica et al. 2009a,b, Cuesta-Martínez et al. 2015a,b)

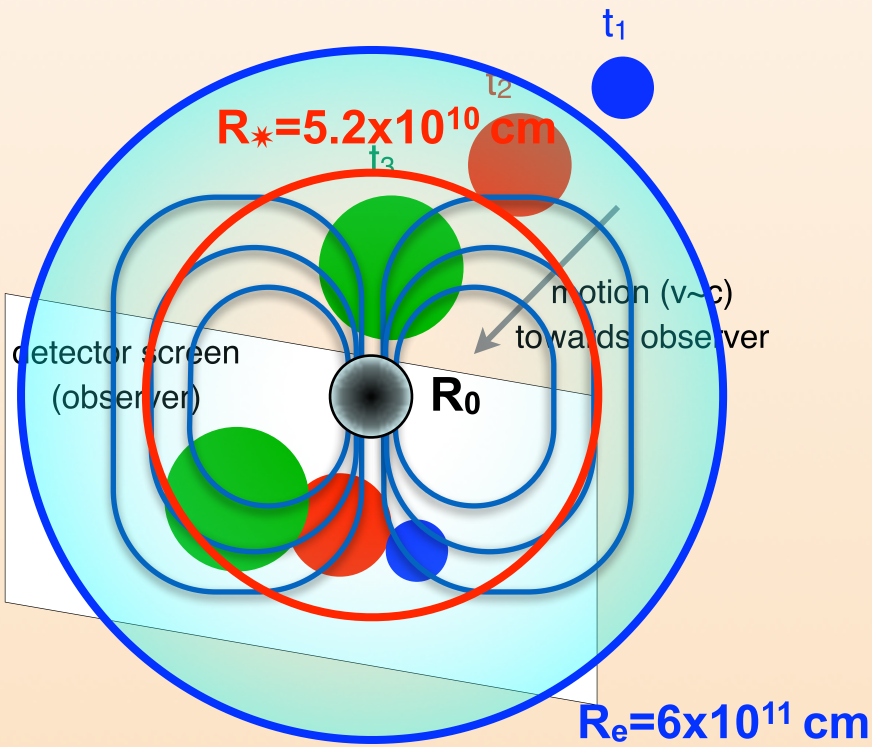

1. Stellar Model: **35OC** (Woosley & Heger 2006). **R* = 5.2x10^{10} cm**
2. RMHD code (MP5, CT, Self-gravity): finite-volume, Eulerian formulation.
3. EoS Table:
   - $\rho > 10^{-4}$ gr/cm^3: Helmholtz EoS (leptonic table + baryons)
   - $\rho < 10^{-4}$ gr/cm^3: baryons + Boltzmann e-gas +radiation.
4. Injection nozzle @ $R_0 = 10^9$ cm.
5. Domain: **[R_0, 6x10^{11} cm] x [0º,90º]** with standard resolution 2560 x 360.
6. Progenitor magnetic field (if any): dipole with a generating current at 2x10^8 cm

Models

Model	B	B	σ	L	ρ	Γ	ε	Ω
B0	0	0	0	6.65	0.1	5	80	0
Bp	0	2	0,18	6.66	0.1	5	80	0
Br	10	0	111	13.7	0.1	5	80	0
Brp	10	1	111	13.7	0.1	5	80	0
ML-4	10	1	107	6.65	0.1	5.03	80	20
ML-5	11	2	27	27.0	0.4	10.07	20	20

Reference jet parameters (nozzle):

- $\theta = 10^{o}$ $\theta\Gamma = 0.87 < 1$ (causally connected)
- $\Gamma = 5$ ($\Gamma_{\infty} \sim 500$)
- $\varepsilon = 80\ c^2$
- $\rho = 0.1$ gr/cm^3
- $p = 2.23 \times 10^{22}$ erg/cm^3

Jet dynamics

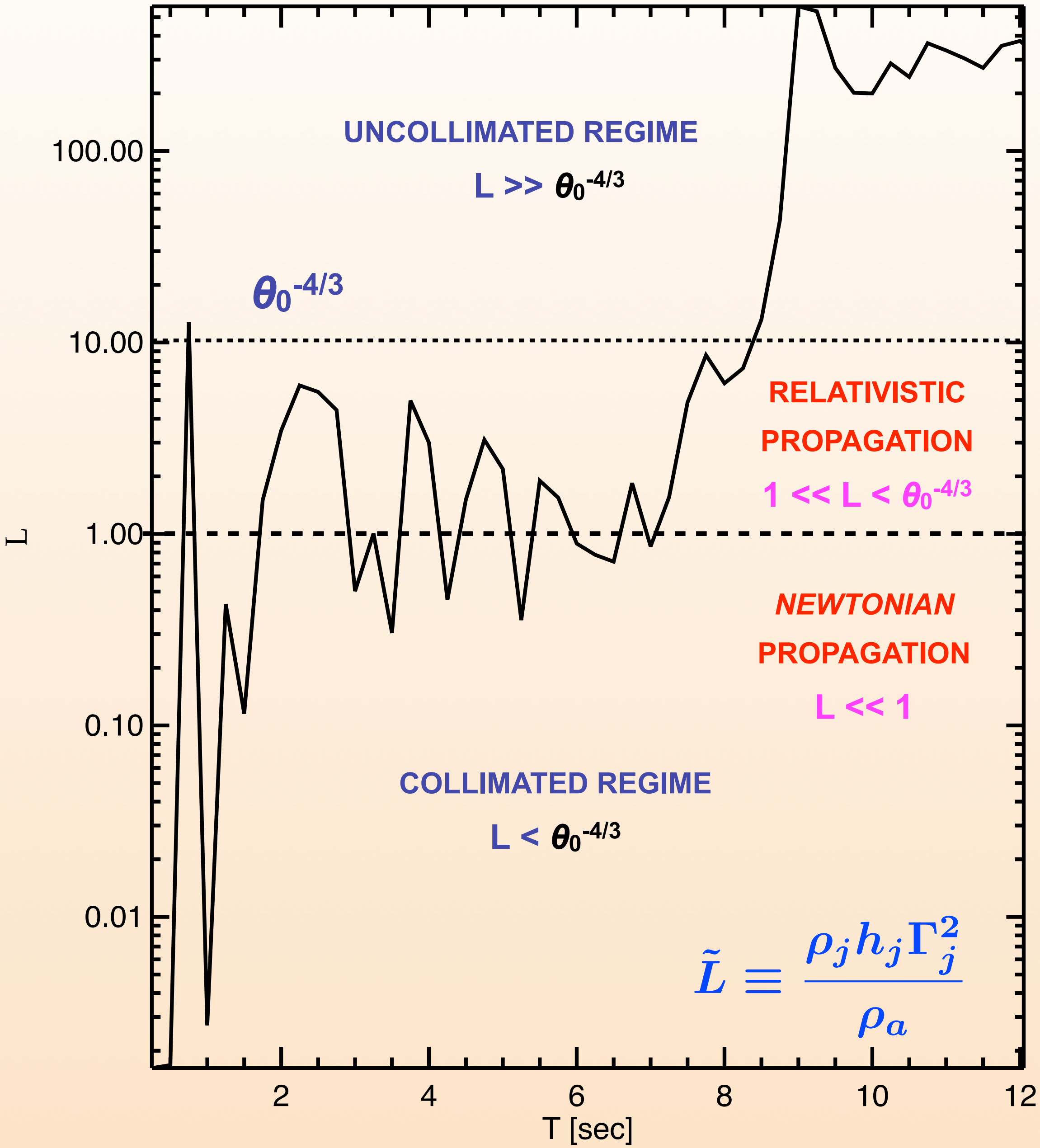

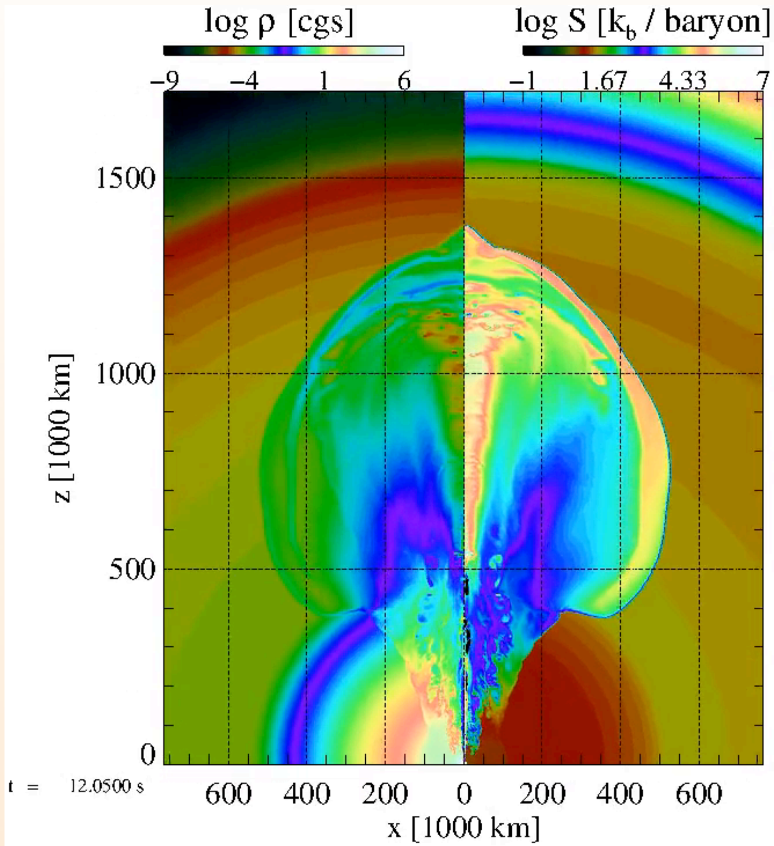

L ~ 1 for most of the propagation inside the progenitor:

- Bromberg+11 analytic estimates (unmagnetized model) are difficult to apply. Particularly when the density decays faster close to the surface.
- The jet is collimated before breakout, and uncollimated after breakout (in agreement with Bromberg+11).

Jet dynamics

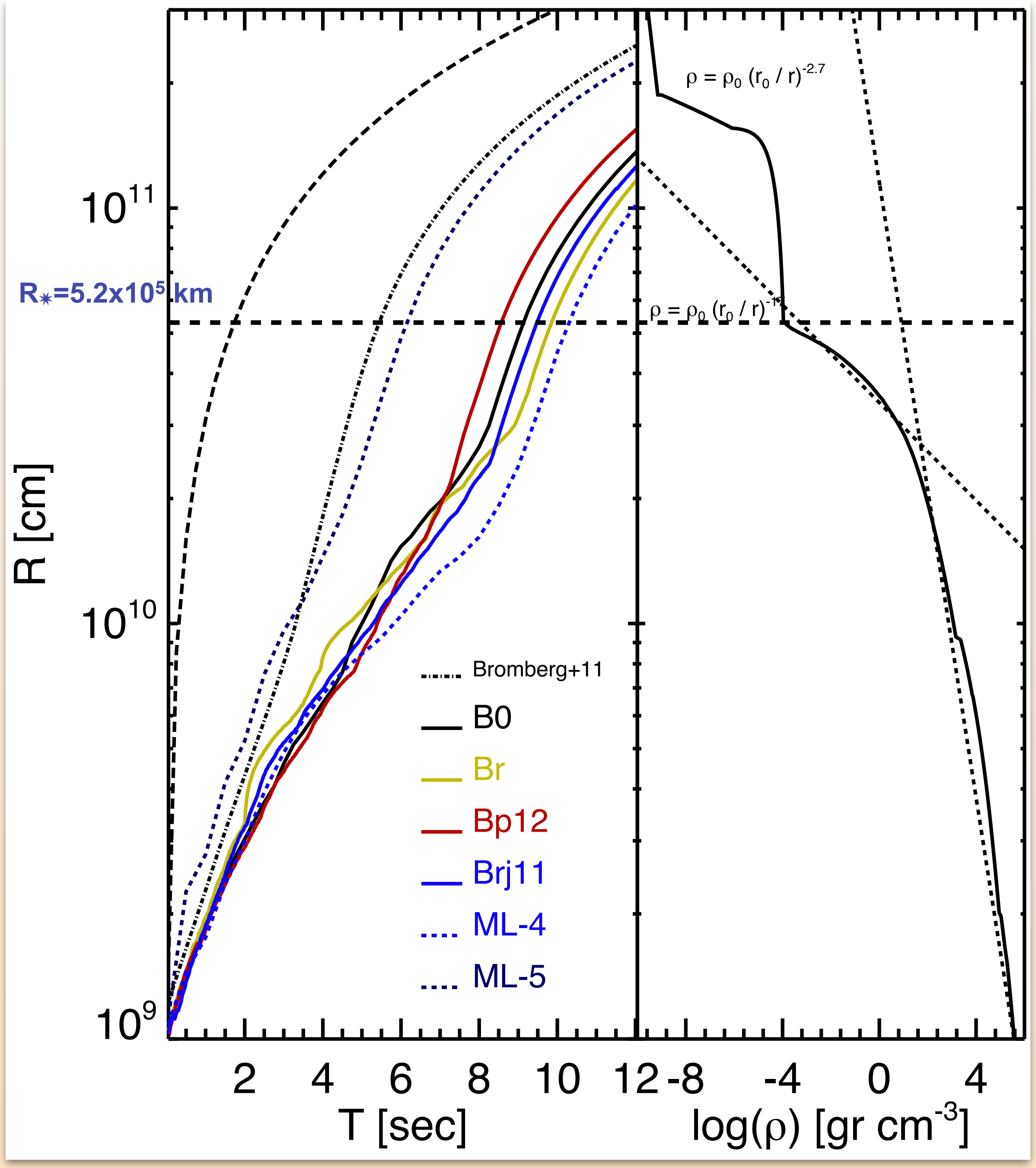

There is not a clear trend for the propagation speed:

- **Faster: model with the largest initial Lorentz factor and jet density (model ML-5; Γ_0=10)**
- **Slower: magnetized models with smaller Bϕ (v~0.33c)**
- **Unmagnetized model: v~0.38c**

Bromberg et al. (2011) estimate (unmagnetized model):

- **Predicts a crossing time of the star of ~5.5 sec, speed 40% larger than the crossing time of model B0 (~9 sec).**
- **Actually, it is shorter crossing time than any other of our models (including magnetic models).**

Jet dynamics

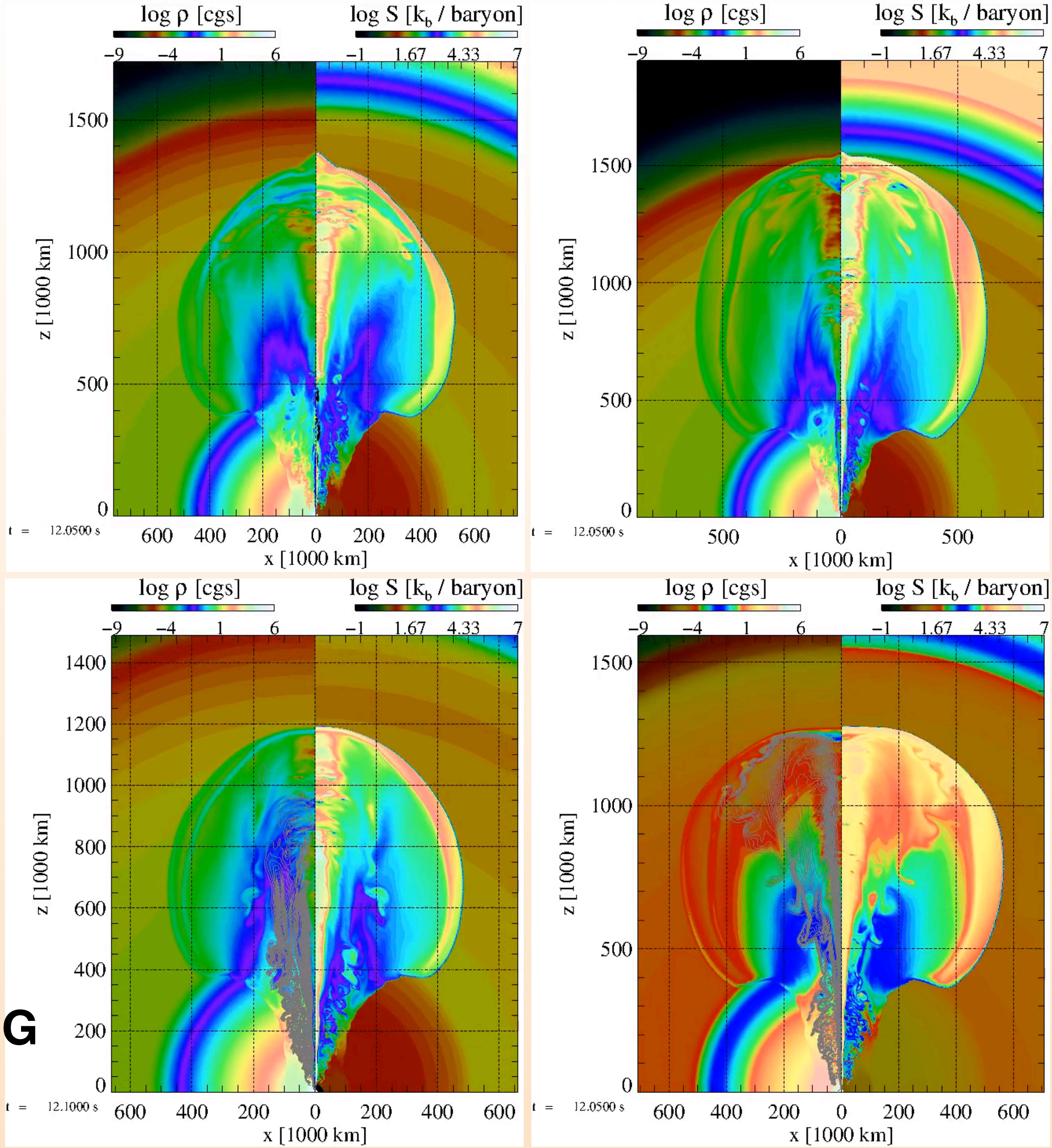

B=0

B_ϕ = 2x10^{10} G
B_{ext} = 0
σ = 0.18

B_ϕ = 0
B_r = 10^{11} G
σ = 111

B_ϕ = 10^{10} G
B_r = 10^{11} G
σ = 111

Jet variability

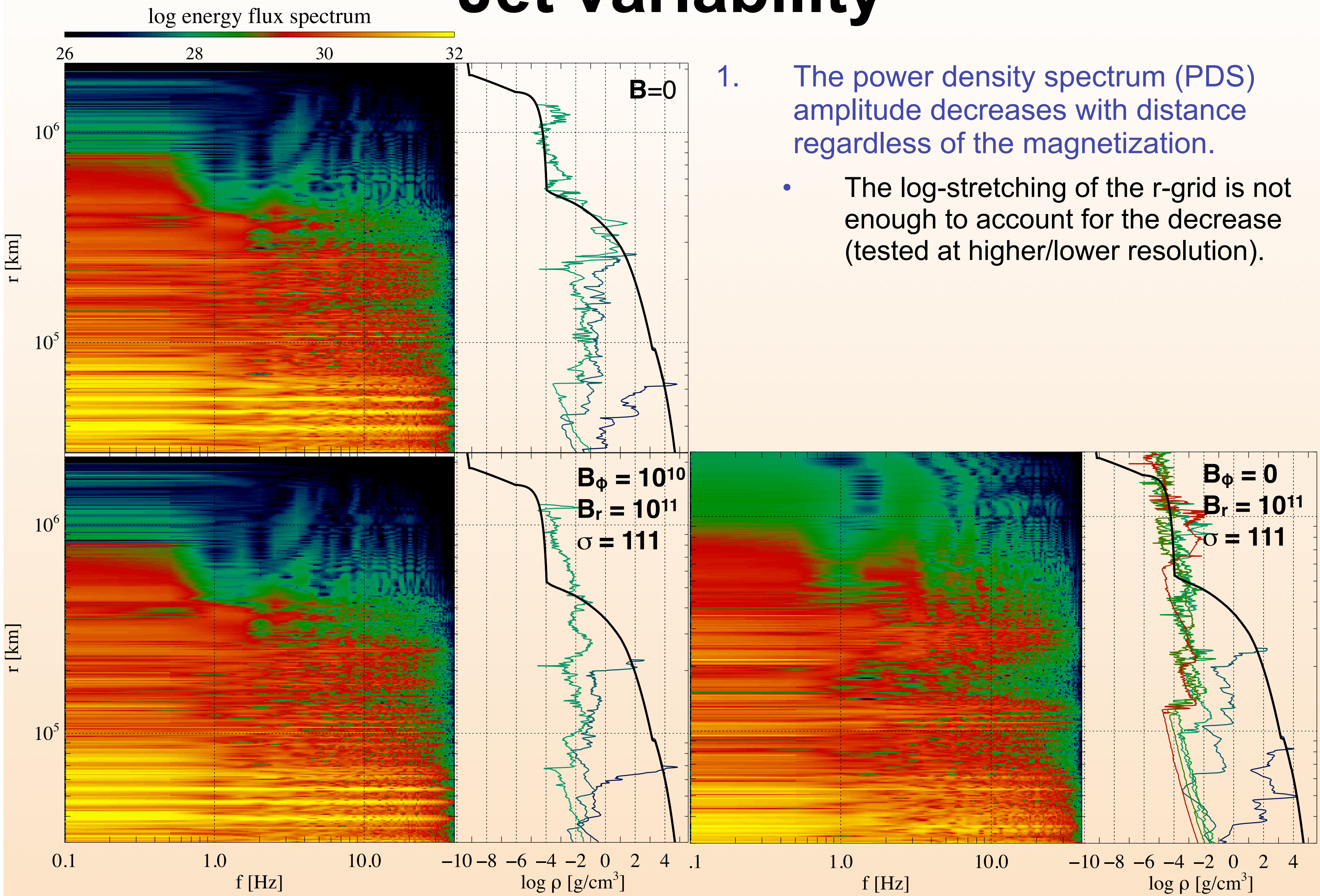

1. The power density spectrum (PDS) amplitude decreases with distance regardless of the magnetization.
   - The log-stretching of the r-grid is not enough to account for the decrease (tested at higher/lower resolution).

Jet variability

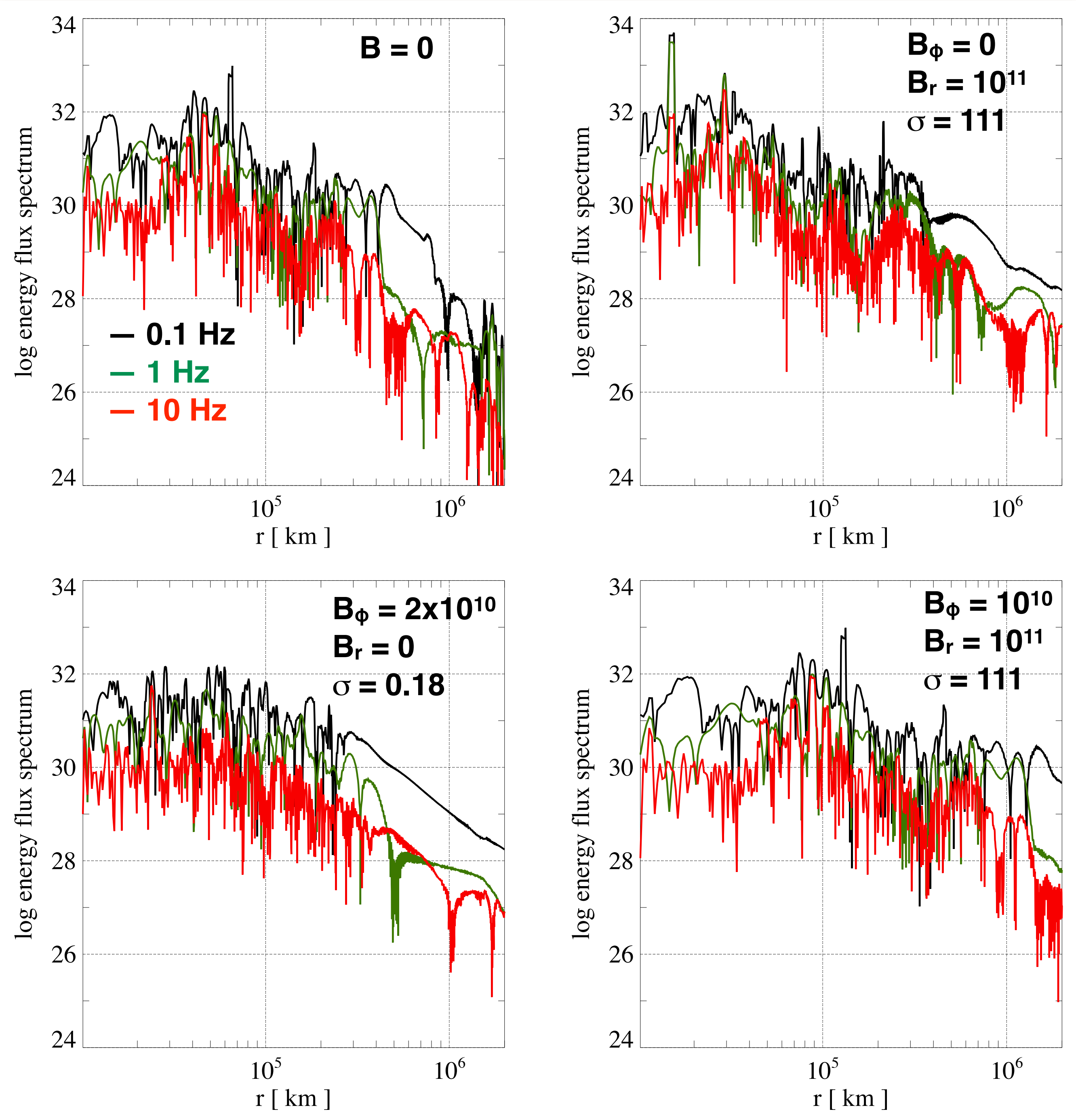

2. **In magnetized models the PDS decrease with distance is smaller.**
   - The most magnetized model with mixed poloidal +toroidal field is the one less affected by the stellar density gradient.
3. **Models with purely toroidal and strong fields show smaller power at high frequencies** (>5 Hz).

Jet variability

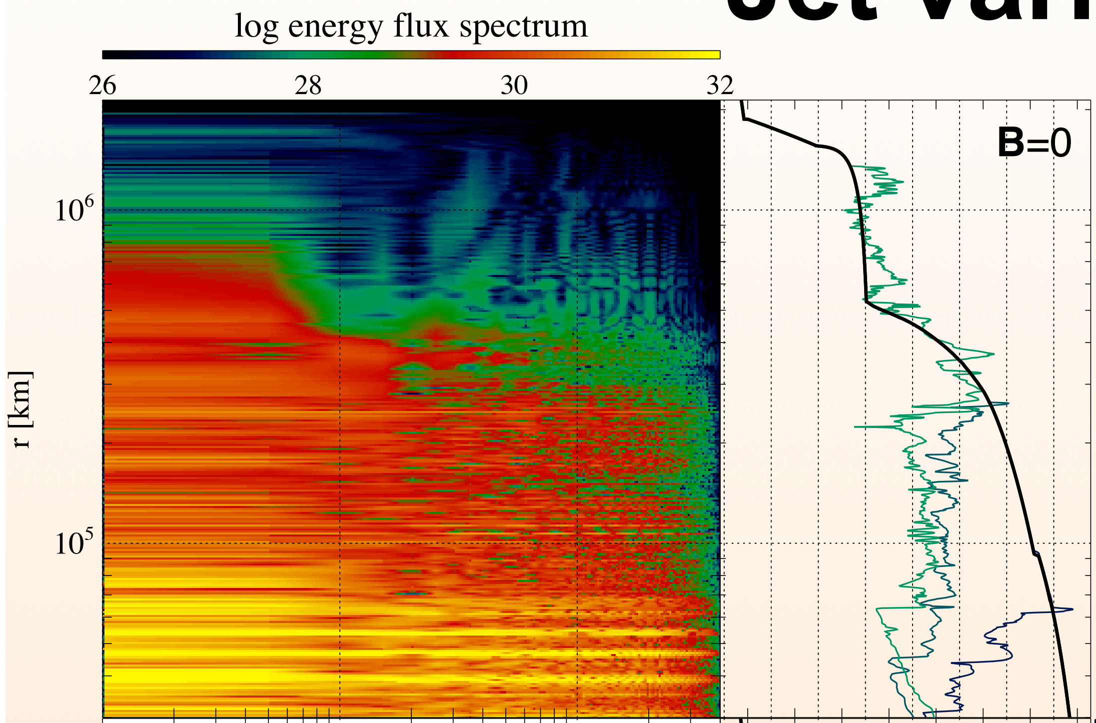

4. The PDS damping occurs chiefly close to the stellar surface, where the steepest density gradient is found.
5. *Provisional:* The acceleration post-break out might damp the high-frequency PDS.
   - Note: We consider in the spectrograms ALL matter regardless its Γ_∞.

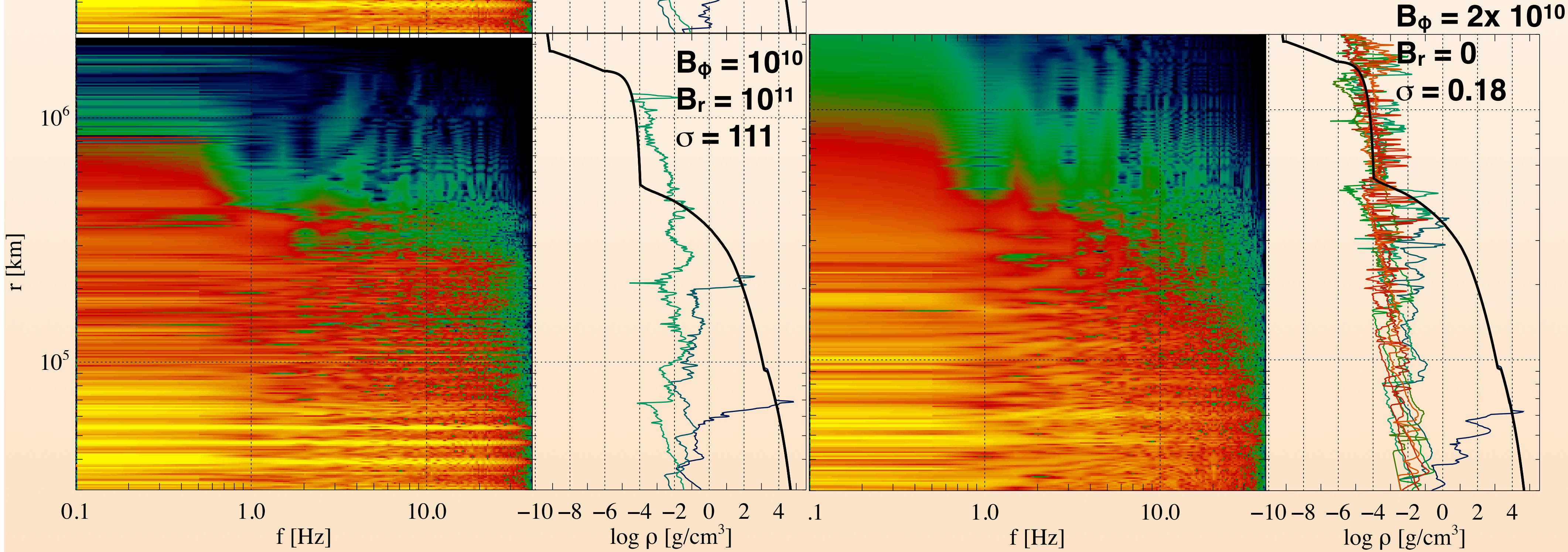

Jet variability

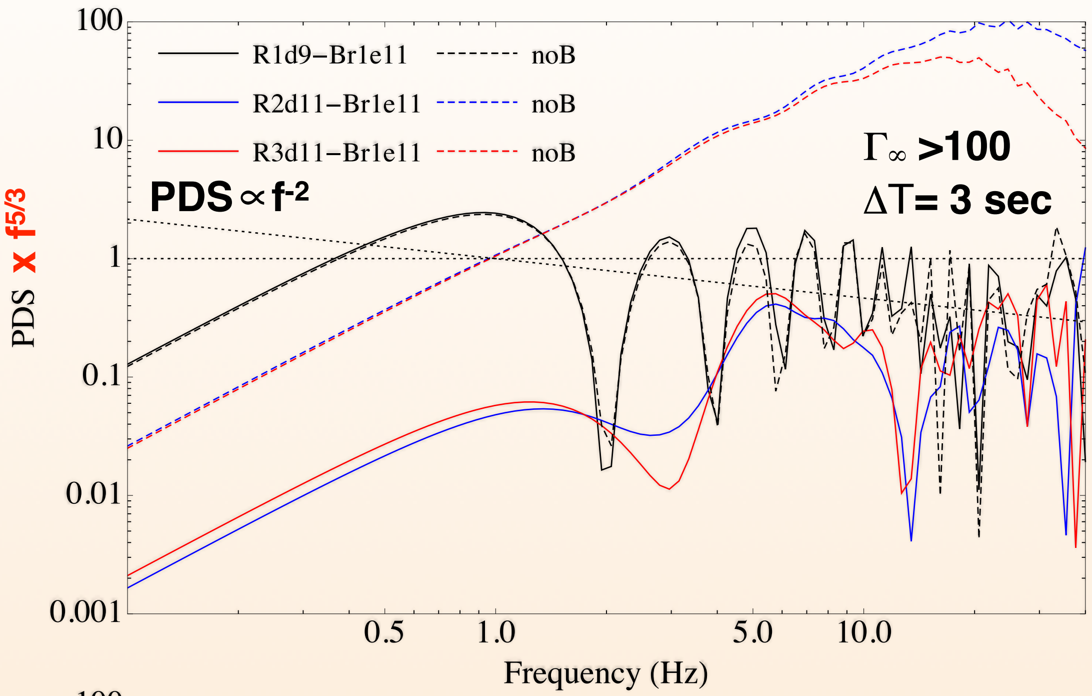

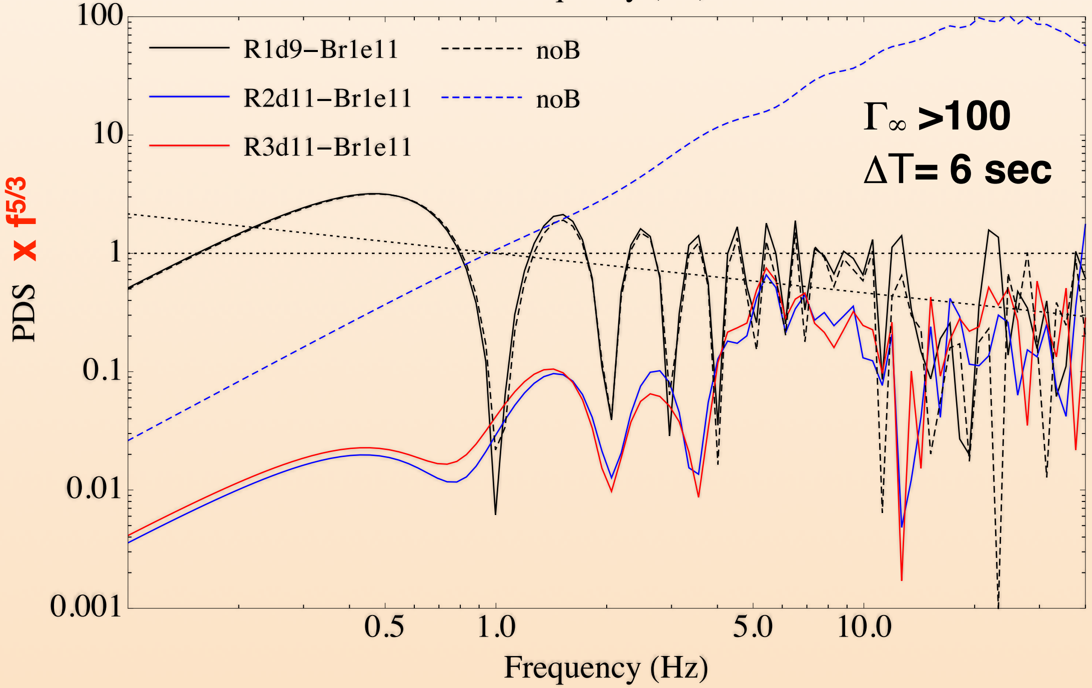

6. Restricting the analysis to matter with Γ_∞>100, magnetized models display smaller PDS at large radii (>2x10^{11} cm) than the non-magnetized one.

    - The peak of the PDSx$f^{5/3}$ happens at f~20Hz for the unmagnetized model, while the PDS ∝ $f^{-5/3}$ in the Brp case.

7. Including in the PDS longer sampling times (ΔT=6 s), obviously raises the low frequency strength, and a minor increase of the power at high frequencies.

Jet variability

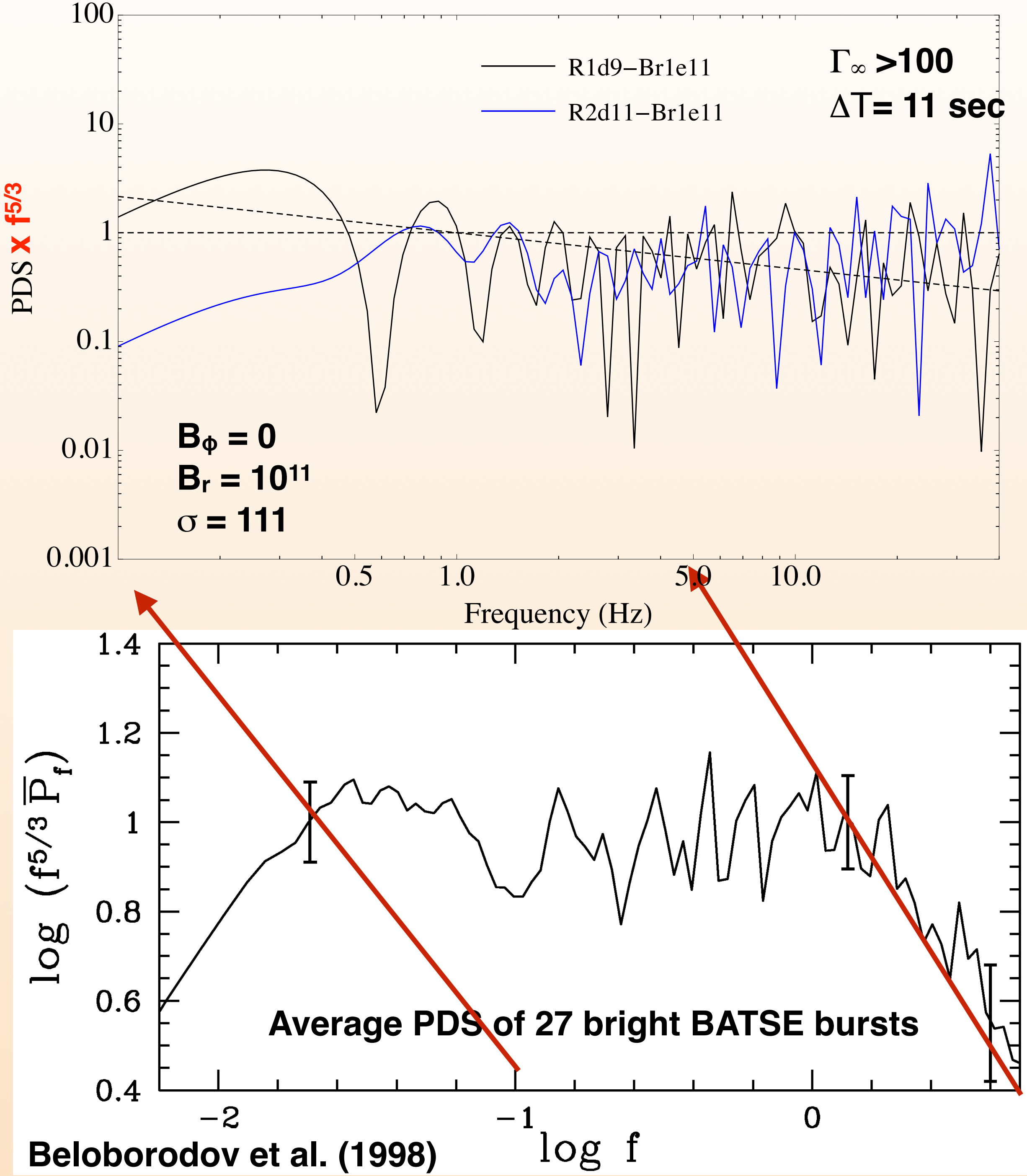

8. In the model with purely poloidal field, we have considered a longer sampling interval (ΔT=11 s). We observe that the PDS at 2×10^{11}

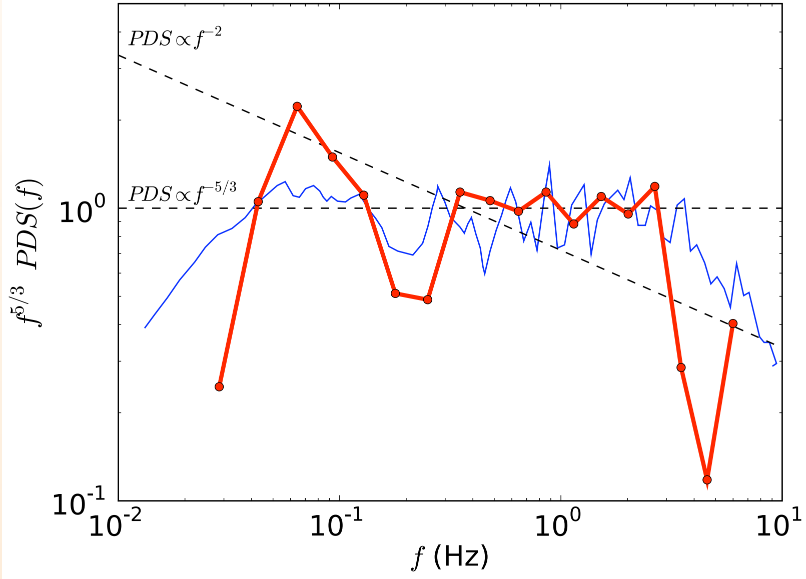

- *We do not expect a one-to-one matching, because the GRB variability may result from a complicated interplay between the variability properties of the flow + emission model.*
- *See, however, Morsony, Lazzati & Begelman (2010)*

Summary and conclusions

- We are exploring the properties of relativistic magnetized jets propagating in collapsars, and (obviously) found that the magnetic field strength and topology can be key to shape both the dynamics of relativistic outflows and their observational signature.

- The jet / star interaction produces a highly variable jet, and the variability PDS depends, in a non-trivial way, on the progenitor structure, as well as on the magnetic field.

- Regardless of the magnetization, there is a decrease of the PDS at high frequencies that we (tentatively) relate to the stellar density gradient.

  - The initial (<5 sec) jet variability may be used as a probe of the structure of the final edge of the star assuming that the LC of a GRB is produced by photospheric emission.

- Provisional: differences in variability at low (<~ 5 Hz) and high (<~ 5 Hz) frequencies can be used as proxy for magnetization.